

Precise Subcellular Input Retinotopy and Its Computational Consequences in an Identified Visual Interneuron

Simon P. Peron, Peter W. Jones, and Fabrizio Gabbiani

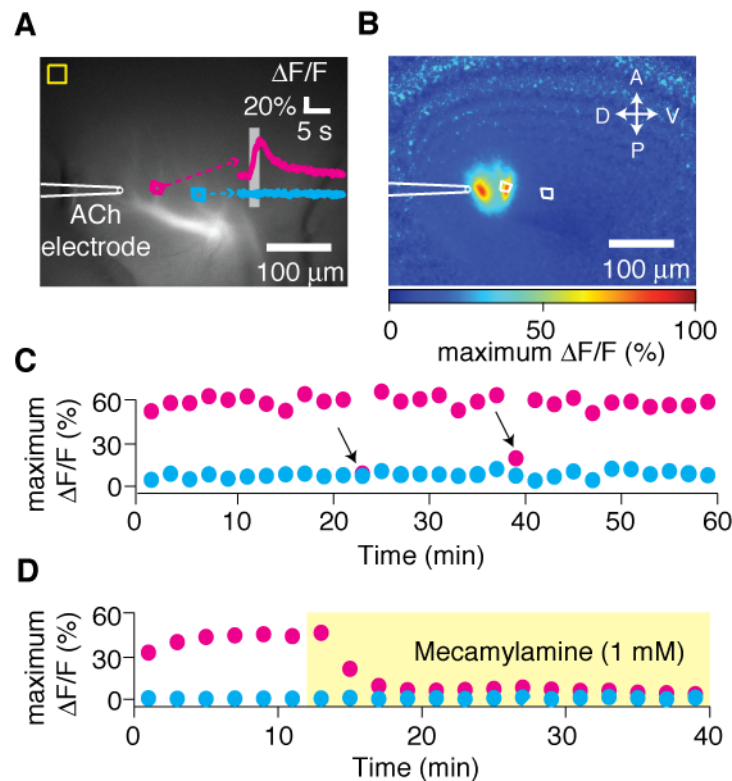


Figure S1. The LGMD's excitatory dendrite possesses calcium permeable nAChRs. (A) Background fluorescence image of an LGMD neuron filled with Oregon Green BAPTA-1 (OGB-1) and employed in an ACh iontophoresis experiment. The yellow square indicates the region employed for background subtraction, and magenta and blue denote the ROIs whose $\Delta F/F$ traces in response to a 2 s ACh stimulus are shown in the inset. The time of ACh ejection is shown in light gray. (B) Maximal $\Delta F/F$ at each pixel during ACh iontophoresis for the same field of view as in (A). Only the two dendritic branches immediately proximal to the electrode showed a calcium response. (C) Response to ACh stimuli administered every two minutes over an hour for the two ROIs shown in (A). Arrows point to the two trials for which motion could be observed; such trials were excluded from subsequent analysis. (D) Response to ACh stimuli spaced every 2 minutes for another cell, with the magenta and blue points indicating the response at an ROI proximal and distal to the iontophoretic electrode, respectively. The yellow region indicates the time following the addition of the nicotinic antagonist mecamylamine (1 mM) to the bath.

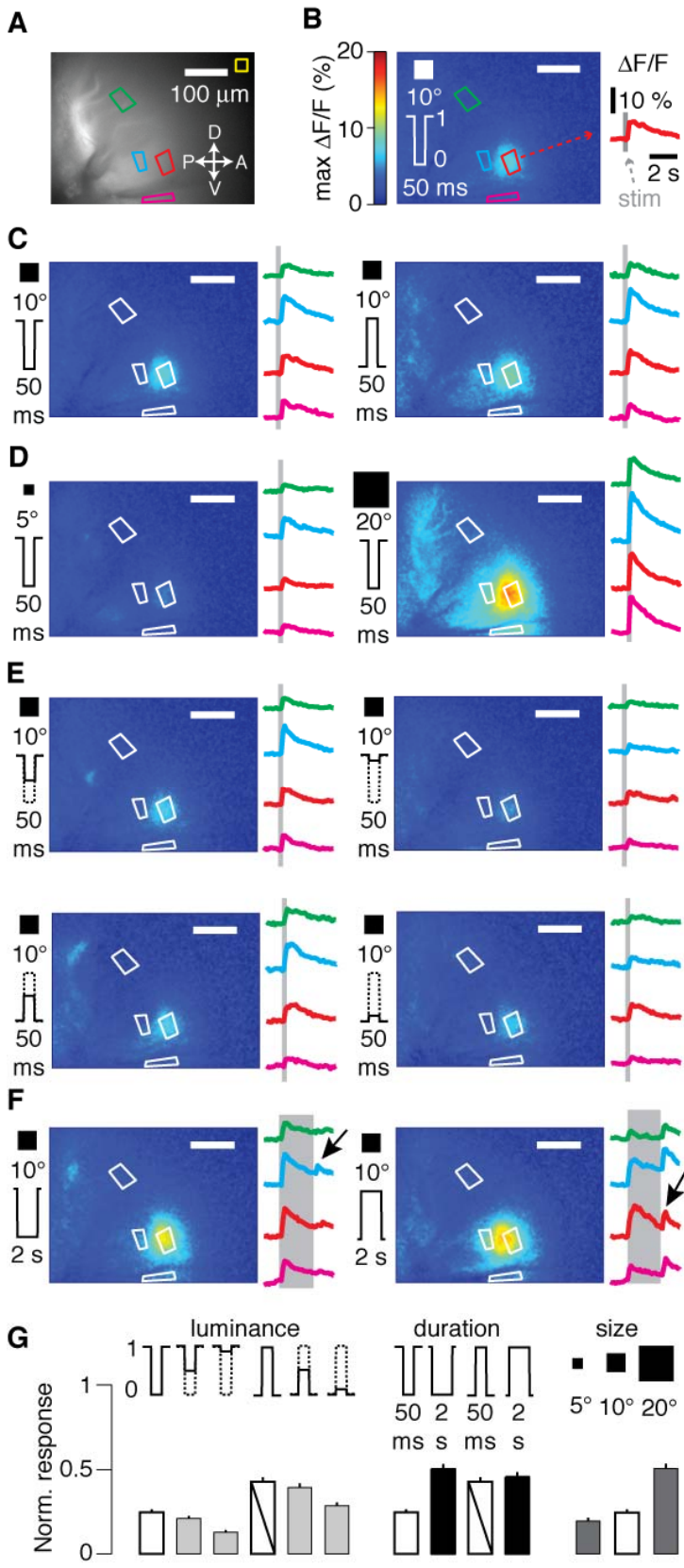


Figure S2. Ca^{2+} response in the LGMD's excitatory dendrite depends on stimulus class and position. (A) Background fluorescence image of an OGB-I filled LGMD neuron employed in a visual stimulation experiment. The yellow square corresponds to the region used for background subtraction while the four colored rectangles denote the ROIs used to calculate $\Delta F/F$ in subsequent panels. The cyan ROI was employed for posterior stimuli (elevation, azimuth: 0° , 120° ; center), and the red, green, and magenta ROIs were employed for anterior (0° , 60°), dorsal (30° , 90°), and ventral (-30° , 90°) stimuli, respectively (see Figure 1 and Krapp and Gabbiani, 2005 for coordinate convention). Arrows denote presumed source of synaptic input in visual space (see Figure 1). Anatomically, dorsal and ventral are the same as the input projection, while anterior and posterior correspond to lateral and medial positions, respectively. (B) Maximal $\Delta F/F$ for each pixel in response to an anterior visual stimulus consisting of a 10° -by- 10° OFF flash lasting 50 ms. The raw $\Delta F/F$ trace for the anterior ROI is shown in red. The time of the stimulus is shown in grey. (C-F) Example maximum $\Delta F/F$ for anterior stimulation along with raw $\Delta F/F$ for a sample trial at each of the four positions in response to various visual stimuli. Stimuli consisted of 50 ms light flashes for (C-E), with 10° -by- 10° ON and OFF flashes shown in (C) – i.e., spanning the entire luminance range of the projector. The responses to OFF flashes for 5° -by- 5° and 20° -by- 20° squares are shown in (D), while (E) shows the responses to 10° -by- 10° squares with varying luminance changes: from left to right, and top to bottom, 100% to 50%, 100% to 90%, 0% to 50%, and 0% to 10% (all percentages in terms of projector luminance relative maximum; see Experimental Procedures for exact luminance values). Finally, the responses to 2 s 10° -by- 10° ON and OFF flashes are shown in (F). (G) Summary data across five animals for all stimulus classes showing normalized maximum $\Delta F/F$ pooled across ROIs (each ROI-animal combination was normalized to its maximum $\Delta F/F$; $N=53$ trials total, with bars indicating mean of this pool; lines indicate pool s.e.m.). The response to a 10° -by- 10° OFF flash lasting 50 ms is shown in all three groups (white outlined with black), and the response to a 10° -by- 10° ON flash is shown twice (white with black slash). For the 10 unique stimuli shown, 40/50 pairwise relationships differed at the $p < 0.01$ significance level based on a Wilcoxon rank sum test. The following 10 did *not* (stimuli are 10° -by- 10° , 50 ms unless otherwise indicated): OFF vs. 100% to 50%, and 0% to 10%; 100% to 50 vs. 0% to 10%; ON vs. 0% to 50%, 2s OFF, 2s ON, and 20° -by- 20° OFF; 2s OFF vs. 2s ON, and 20° -by- 20° OFF; 2s ON vs. 20° -by- 20° OFF.

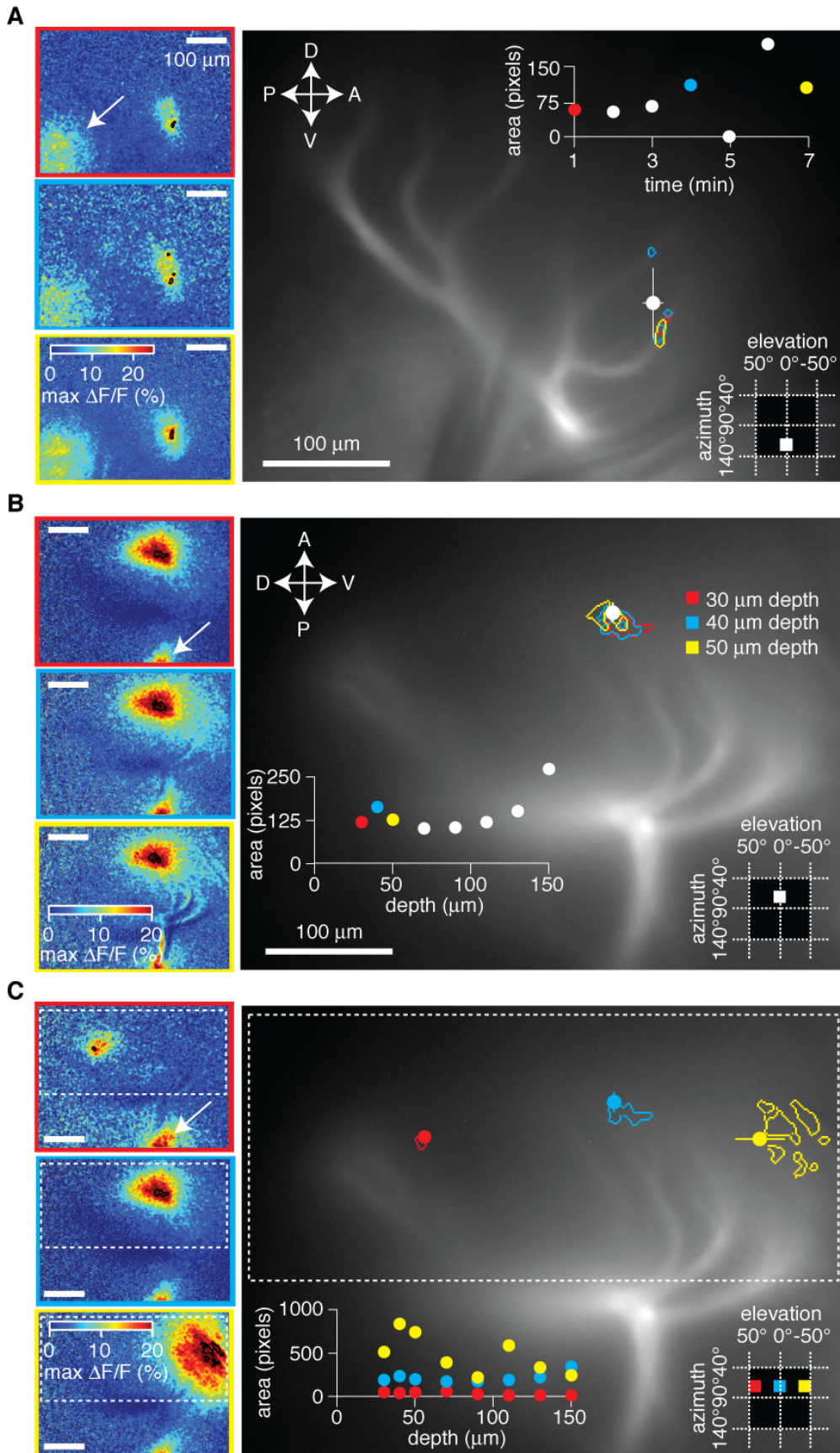


Figure S3. The center-of-mass (COM) for the set of pixels that attain or exceed 85% of the overall maximal $\Delta F/F$ for a given visual stimulus has a low variability across stimulus repetitions and imaging depth, and exhibits this stability across the entire viewing area. (A) Response variability as a function of time. The same 20°-by-20° OFF square was presented in one minute intervals and imaged at the same depth. The three left panels show sample raw maximal $\Delta F/F$ for three trials, with the region representing pixels whose maximal $\Delta F/F$ attained or exceeded 85% of the overall maximum $\Delta F/F$ outlined in black. The arrow in the top left panel points to the calcium signal originating near the spike initiation zone (SIZ), responsible for spike-frequency adaptation (Peron and Gabbiani, 2009a); this signal was ignored. The right panel shows a background fluorescence image of the same OG BAPTA-I neuron as in the left three panels. The regions attaining or exceeding 85% of maximal $\Delta F/F$ from the three trials in the left panels are outlined in the same color as those panels' frames. The COM is shown in white, with SD lines, and is the average of several repetitions (N=7). The inset shows the area of each of the seven trials, with the color-coded trials corresponding to those shown in the left panels. Though areal variability was high, COM position was stable. The directional arrows (anterior, posterior, dorsal ventral) correspond to the position in visual space of the incoming inputs from the eye (see Figure 1). The inset with the white square shows the position of the stimulus in visual space. (B) Response as a function of depth. The same 20°-by-20° OFF square was presented in 250 s intervals and imaged at different depths. Same conventions as in (A). COM was averaged across depths, with lines indicating SD (N=8). (C) Response as a function of depth for three positions. 20°-by-20° OFF squares were presented in 250 s intervals at three positions and imaged at different depths. Same conventions as in (A). The panels on the left show the response at the shallowest (30 μm) depth for each position. The dotted lines indicate the subregion that was used to apply the $\Delta F/F \geq 85\%$ criteria; this was done to omit the calcium influx from the SIZ (see Experimental Procedures). The inset in the right panel shows the area as a function of depth for the three stimulus positions; areas below 10 pixels were automatically assigned an area of 0 and omitted from subsequent analysis. The inset with the colored squares shows the positions, in visual space, of the three stimuli. Color-outlined regions correspond to those from the panels on the left; these are single example trials, and not the entirety of the pixel set from which COM position was computed.

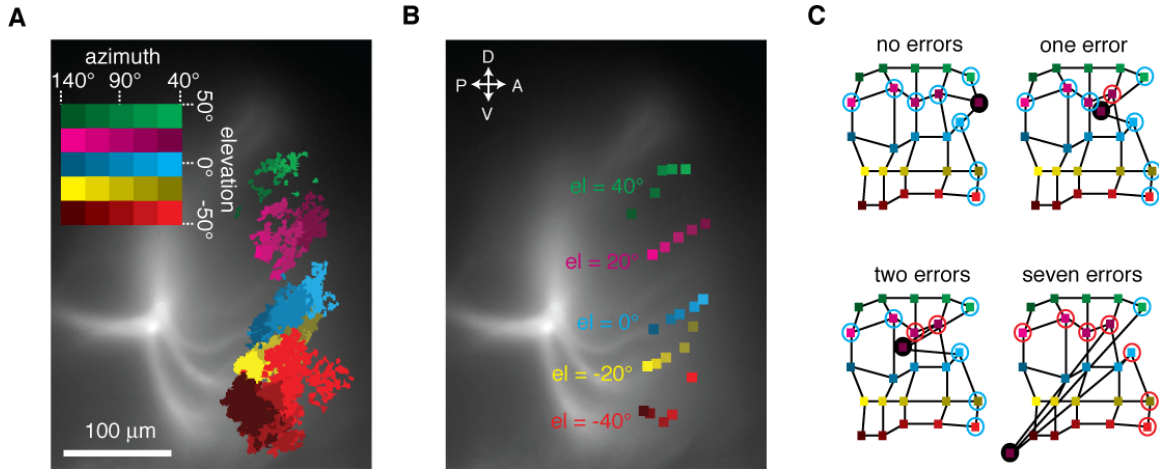


Figure S4. Algorithm employed to quantify the degree of retinotopy at the level of the dendrites. (A) Raw responses to distributed stimuli in an LGMD neuron imaged from a single field-of-view and 10 depths. OFF stimuli were employed across a 100°-by-100° area divided into a grid of 25 20°-by-20° squares. The color code in the inset (coordinates given are in visual space) matches the color of the fluorescence response superimposed over the raw OGB-I fluorescence image. (B) Centers-of-mass (COM) for the responding regions shown in (A). Directional arrows (anterior, posterior, dorsal ventral) correspond to the position in visual space of the incoming inputs from the eye (see Figure 1). (C) Sample COM grid demonstrating methodology for computing retinotopy violations. For a given COM (in this example, the purple point on a black background), its relationship to all neighboring COMs sharing the same input stimulus azimuth or elevation was assayed, for a total of eight comparisons. In each of the four error conditions shown (zero, one, two, and seven errors), the points against which comparisons were applied are circled; a blue circle indicates a correct relationship, while a red circle indicates an erroneous relationship. A relationship was considered erroneous if the ordering of the two COMs along the dorso-ventral or anterior-posterior axes did not match the ordering along elevation or azimuth, respectively, of the visual stimuli. Since there are 8 tests per point (4 each along the anterior-posterior and dorso-ventral axes), a 25 point grid has 200 tests. As this scheme counts the test between any two points twice, there are actually 100 unique tests in the 25 point grid used for coarse and fine mapping.

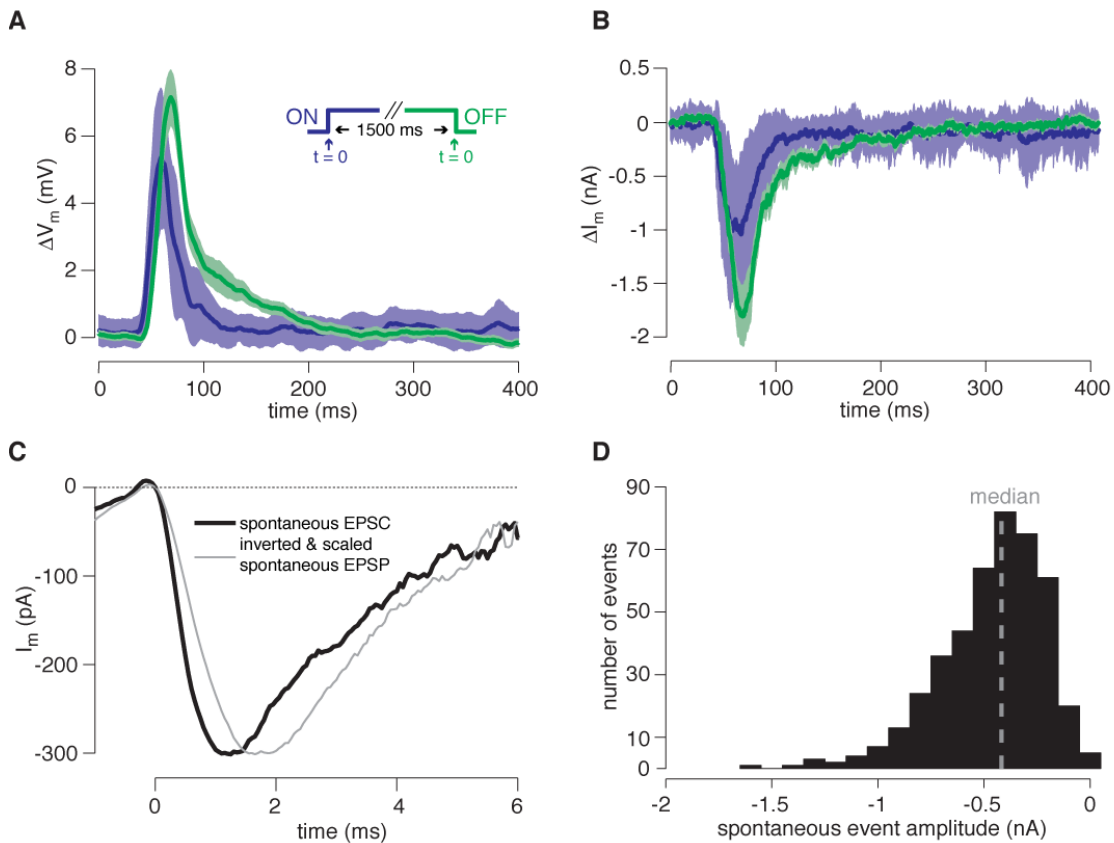


Figure S5. Single ommatidium stimulation elicits a response constituting ~5 LGMD input afferents. (A) Average ON (blue) and OFF (green) intracellular V_m responses to presentation of a 1500 ms light flash. Time 0 is defined as the time of flash onset or offset. Mean responses with s.e.m. envelope are shown, with $N=19$ and 10 distinct ommatidia averaged for OFF and ON stimuli, respectively (gathered from 5 animals). Stimulation yielded mean peak ON and OFF membrane potential deflections of 6.37 and 7.80 mV, respectively. (B) Voltage clamp data showing mean current (nA) during single ommatidium stimulation for same 5 animals as in (A). In this case, $N=17$ and 13 distinct ommatidia are included for OFF and ON responses, respectively. Color and stimulus scheme as in (A). Stimulation yielded mean peak ON and OFF currents of -1.78 and -2.32 nA, respectively. (C) Average spontaneous event in the LGMD measured in both voltage clamp (I_m ; black) and current clamp (V_m ; grey) in one representative recording. (D) Distribution of spontaneous EPSC amplitudes used to estimate the spontaneous event size for the same experiment as in (C) ($N=442$ events). Median and mean values were -0.42 and -0.46 nA, respectively. These events are likely synaptic currents driven by single spontaneous spikes in the afferent population, as application of TTX onto the excitatory dendrite abolishes these membrane responses, ruling out spontaneous vesicular fusion. Estimation of the number of inputs activated by stimulation of a single ommatidium is thus performed by dividing the peak height of the stimulus response by the median spontaneous event height. Peak currents, rather than current integrals, were used because the compound EPSC evoked by single ommatidium stimuli is much longer than the average spontaneous event (>50 ms versus ~5 ms), making it likely that the afferents are firing multiple spikes in response to the stimulus. However, the rising phase

of the EPSC is very sharp in single trials and occurs with a consistent latency, meaning that the peak of the response should reflect the summation of currents from the near simultaneous afferent response. Thus, dividing the current integral by the mean spontaneous EPSC integral will approximate the number of presynaptic spikes, without the ability to distinguish presynaptic neuron number, while dividing peak current by mean spontaneous EPSC amplitude should reflect the number of inputs – i.e., presynaptic neurons. In this way, we obtain an estimate of 5.44 ± 0.46 and 4.64 ± 0.37 (mean \pm s.e.m.) inputs per ommatidium for OFF and ON stimuli, respectively. The estimates for number of afferents activated by OFF and ON stimuli are not statistically distinct (p-value for OFF vs. ON: 0.36, Wilcoxon rank-sum).

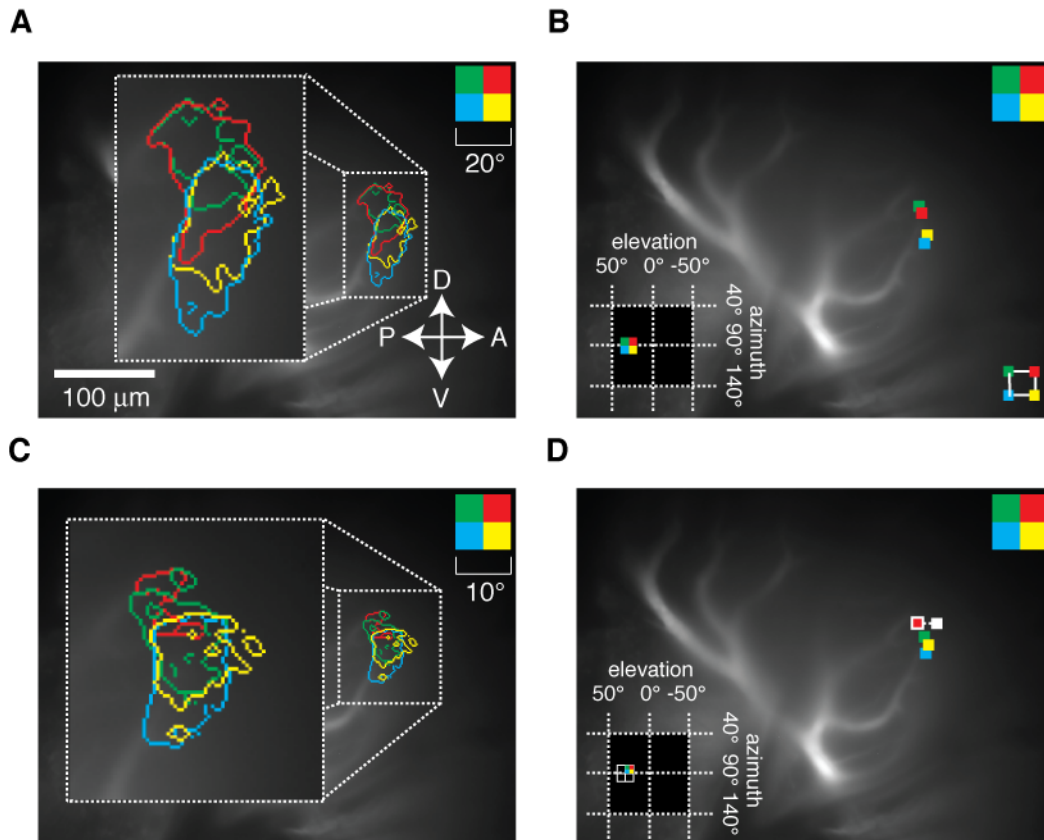


Figure S6. The excitatory dendritic field's inputs preserve retinotopy at the intermediate scale. (A) Raw responses to 4 adjacent 10°-by-10° square OFF stimuli. The color code in the inset matches the color of the fluorescence response superimposed over the raw OGB-I fluorescence image. The pixels whose $\Delta F/F$ attained or exceeded 85% of the overall maximal $\Delta F/F$ for each stimulus are outlined with the color corresponding to the stimulus position. Directional arrows (anterior, posterior, dorsal ventral) correspond to the position in visual space of the incoming inputs from the eye (see Figure 1). (B) Centers-of-mass (COM) for the responding regions shown in (A). The bottom-right inset shows the comparisons applied to quantify the departure from

retinotopy (see Figure S2, as well as Experimental Procedures). (C) Raw responses to 4 adjacent 5°-by-5° square OFF stimuli. Conventions as in (A). (D) COMs for the responses illustrated in (C). Retinotopy-violating COM is shown in white outline, along with positional shift that would restore retinotopy.

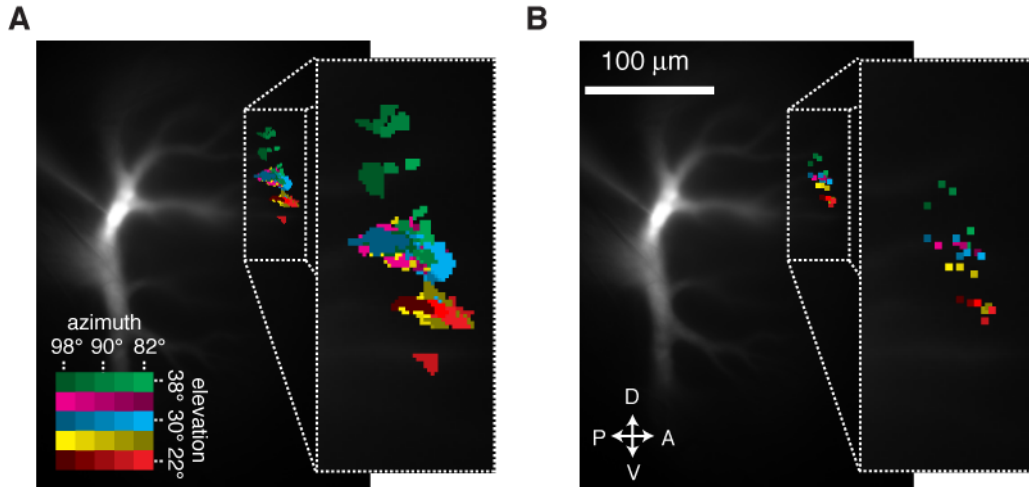


Figure S7. Retinotopy preservation with 0.5°-by-0.5° stimuli spaced 4° apart. (A) Raw fluorescence responses to fine-scale stimuli in the same LGMD neuron shown in Figure 3. The color of the fluorescence response superimposed over the raw OGB-I fluorescence image correspond to color code in inset. The stimuli were 50 ms 0.5°-by-0.5° ON stimuli, spaced 4° apart, and did not fill the full inter-stimulus space. Five repetitions were performed at a single imaging depth. For each trial, the pixels with $\Delta F/F \geq 85\%$ of the overall maximal $\Delta F/F$ were recorded; each colored area corresponds to the union of such pixels across trials for a given stimulation site (see Experimental Procedures). The inset shows a magnified view of the responding region. (B) Centers-of-mass (COM) for the responding regions shown in (A).

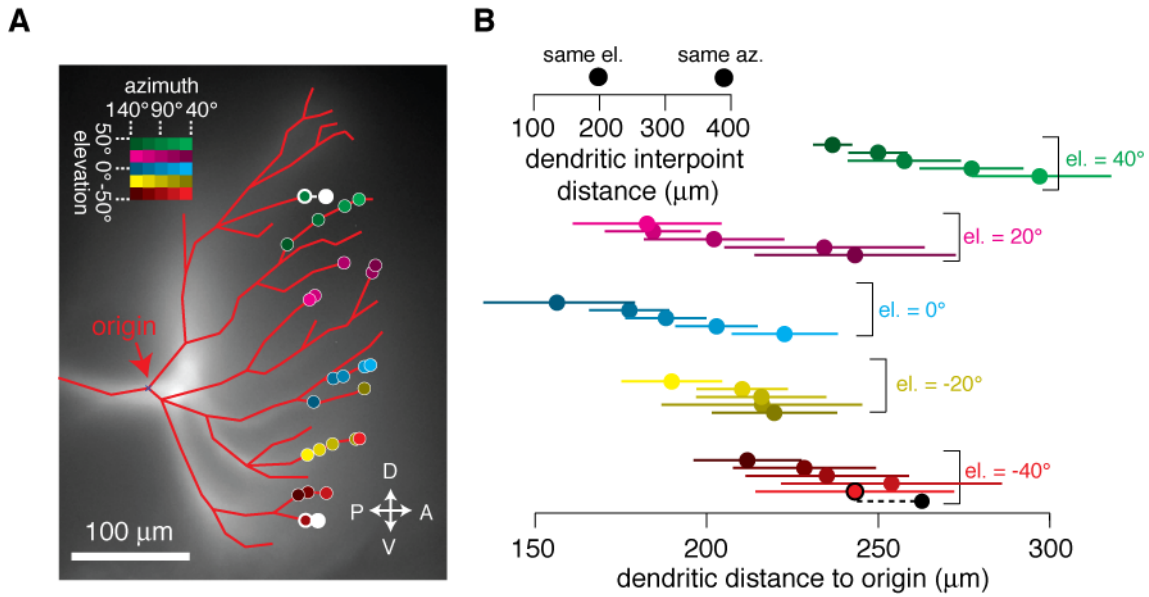


Figure S8. Stimuli having the same elevation activate synapses that are dendritically closer relative those having the same azimuth. (A) Dendritic tracing (red lines) of an LGMD neuron superimposed on a raw fluorescence image. Each colored point is placed on the dendritic point closest to its corresponding COM (from Figure S4B). The red arrow points to the origin of the excitatory dendritic field (i.e., the first bifurcation). The COMs outlined in thick white should be moved to the white circle position to not violate retinotopy. (B) Distance from origin along the dendrite for each of the 25 visual stimuli, averaged across animals (N=7 animals; lines indicate s.e.m.). Inset shows the mean shortest dendritic distance between points whose visual stimuli had the same elevation or azimuth. Dotted black lines show where COMs should shift to so as not to violate retinotopy.

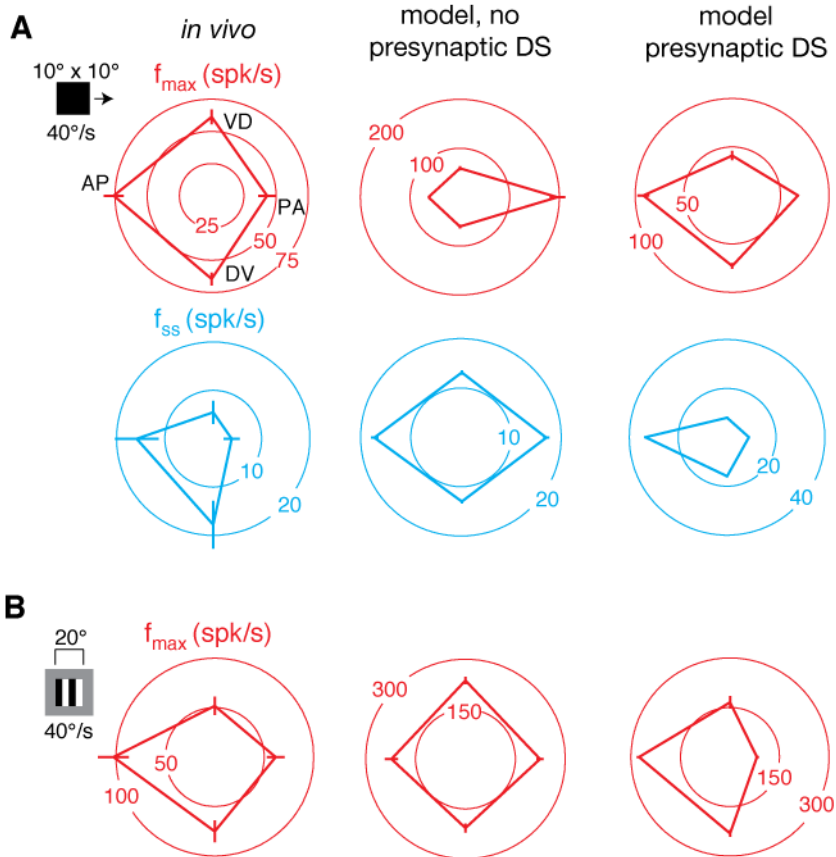


Figure S9. Introducing directional bias at the level of the excitatory input signal reconciles the model’s directional preference with physiological observations. (A) Directional selectivity in the real and model neuron in response to translation by a 10° -by- 10° square. In each case, the response to AP, PA, DV, and VD motion is indicated on the circular plot, with red indicating f_{max} and blue f_{ss} (see Figure 5). The left column shows the *in vivo* LGMD/DCMD response, the middle column shows the response of the model without excitatory input directional bias, and the right column shows the response of the model with this bias. (B) Directional selectivity for the real neuron and the two models in response to drifting gratings. Same conventions as in (A).

Stimulus Size	vertical bars		horizontal bars			p-value (signed rank) horizontal vs. vertical
	f_{max} ($\mu \pm$ SEM; spk/s)	n_{trials}	f_{max} ($\mu \pm$ SEM; spk/s)	n_{trials}	$n_{animals}$	
<i>In vivo</i>						
$80^\circ \times 5^\circ$	42.5 ± 10.0	43	33.0 ± 9.1	43	7	0.03
$20^\circ \times 5^\circ$	35.3 ± 8.0	43	27.1 ± 6.9	43	7	0.02
$10^\circ \times 2.5^\circ$	23.9 ± 7.9	38	27.0 ± 9.2	38	6	0.25
<i>Simulated</i>						
$80^\circ \times 5^\circ$	40.0 ± 0.9	10	20.0 ± 0.7	10	–	–
$20^\circ \times 5^\circ$	37.4 ± 4.9	10	39.4 ± 5.5	10	–	–
$10^\circ \times 2.5^\circ$	24.0 ± 6.7	10	26.6 ± 9.0	10	–	–

Table S1. Responses to vertical and horizontal bars *in vivo* and in simulated LGMD. The leftmost column indicates the size of the stimulus. The second and third columns give the peak instantaneous frequency (f_{max}) response to the vertical bar (spikes/second; mean \pm s.e.m.) and the number of trials used to calculate statistics, respectively. The fourth and fifth columns give the same numbers for horizontal bars. The sixth column indicates the number of animals used for each stimulus class (not applicable to simulation data), while the last column gives the p-value of the signed rank comparison of the f_{max} responses for horizontal and vertical bars.

Response Measured	DI_{AP/PA} ($\mu \pm SD$)	p-value (signed rank)	DI_{DV/VD} ($\mu \pm SD$)	p-value (signed rank)	p-value (rank sum) DI_{AP/PA} vs. DI_{DV/VD}
<i>Translating Squares</i>					
<i>In vivo</i> f_{max}	0.31 \pm 0.27	1.4×10^{-6}	0.04 \pm 0.18	0.22	0.03
<i>In vivo</i> f_{ss}	0.68 \pm 0.25	1.1×10^{-7}	0.48 \pm 0.40	5.4×10^{-6}	9.8×10^{-6}
<i>Model without</i>					
<i>DS</i> f_{max}	-0.49	–	0.01	–	–
<i>Model without</i>					
<i>DS</i> f_{ss}	0.01	–	-0.01	–	–
<i>Model with DS</i>					
f_{max}	0.14	–	0.29	–	–
<i>Model with DS</i>					
f_{ss}	0.58	–	0.33	–	–
<i>Drifting Gratings</i>					
<i>In vivo</i> f_{max}	0.27 \pm 0.20	2.3×10^{-4}	0.15 \pm 0.18	0.01	0.14
<i>In vivo</i> <i>maximal</i> $\Delta F/F$	0.25 \pm 0.16	2.8×10^{-4}	0.25 \pm 0.15	2.8×10^{-4}	0.99
<i>Model without</i>					
<i>DS</i> f_{max}	-0.01	–	-0.07	–	–
<i>Model with DS</i>					
f_{max}	0.54	–	0.19	–	–

Table S2. Directionality indices (DIs) for responses to drifting gratings and translating squares. All indices were computed as $DI_{A/B} = (A+B)/(A-B)$, so a positive value means the response to A is greater. The leftmost column indicates the stimulus class and variable measured; sample size was 10 trials for all simulations, 18 for drifting grating experiments, and 35 for translating square experiments. For gratings, physiological samples (maximum $\Delta F/F$ and f_{max}) were obtained by taking the mean for each position-animal combination and pooling across positions (N=5 animals; usually, 4 positions per animal). For translation, data was simply pooled across animals (N=7 animals; 5 trials each). The second and fourth columns give mean DI's with SD values, and the third and fifth columns give the p-value for the Wilcoxon signed rank test determining if the distribution of DIs differs from zero. No such analysis is performed for simulated responses. The sixth column is the p-value for a Wilcoxon rank sum test between $DI_{AP/PA}$ and $DI_{DV/VD}$. Both the simulations with directional selectivity (DS; see Experimental Procedures) and without DS are included.

Motion Direction	normalized maximal $\Delta F/F$ ($\mu \pm \text{SEM}$)	normalized f_{\max} ($\mu \pm \text{SEM}$)	p-value (rank sum)	absolute change	relative change (%)
<i>AP</i>	0.72 ± 0.03	0.62 ± 0.04	0.07	-0.10	-14%
<i>PA</i>	0.43 ± 0.03	0.36 ± 0.03	0.27	-0.07	-16%
<i>DV</i>	0.65 ± 0.03	0.47 ± 0.03	7.5×10^{-4}	-0.18	-28%
<i>VD</i>	0.42 ± 0.03	0.35 ± 0.03	0.64	-0.07	-17%

Table S3. Change in response for directional drifting gratings due to dendritic filtering. In all cases, data was pooled across all animals and positions (N=53 trials per motion direction, over N=5 animals), though it was normalized to the maximal response at each animal-position combination. The leftmost column indicates the direction of drifting grating motion; gratings moved at 40 °/s. The second column shows the normalized response at the level of the fluorescence signal (maximal $\Delta F/F$). The third column shows the normalized f_{\max} response, with the fourth column indicating the significance of the change between maximum $\Delta F/F$ and f_{\max} . The last two columns show absolute and relative response decline, presumably due to dendritic filtering.